8. Stress Analysis and Crack Growth Rates for Davis-Besse CRDM Nozzles 2 and 3

In this section, we describe the results of the detailed computational fluid dynamics (CFD) modeling efforts that we undertook to develop a better understanding and definition of the thermal hydraulic conditions in the CRDM nozzle annulus and developing wastage cavity at both CRDM Nozzles 2 and 3.

The purpose of these calculations was to determine the thermal-hydraulic conditions that resulted from the leakage of high-pressure, high-temperature reactor coolant through CRDM nozzle cracks into the nozzle annulus and developing wastage cavity. These calculations allowed us to identify the environmental conditions including fluid velocities, temperatures, pressures, steam quality (wetness), and local temperature of the alloy steel RPV head material and CRDM nozzles in the annulus and wastage cavity, as the leakage flow rate increased and as both the CRDM crack and the wastage cavity grew.

These environmental conditions dictate the material removal mechanisms that were responsible for the formation of the wastage cavity. Our results indicate that the flow velocities and thermal conditions were conducive to rapid growth of the wastage cavity. Prior to the Davis-Besse event, the combination of conditions required for rapid material removal by physical and chemical mechanisms were not anticipated by the utility industry or by the NRC to occur in the CRDM annulus. Hence, this cavity wastage was unexpected, unforeseen, and can not be considered ordinary "wear and tear."

Recently available experimental measurements developed by an NRC research program at Argonne National Laboratory (ANL) and published in November 2006 have provided crack growth rate information specifically for the Alloy-600 material from Davis-Besse Nozzle 3. The CGRs measured by ANL for the Nozzle-3 specific material were three to four times faster than those used by EPRI MRP in evaluating CRDM nozzle CGRs due to PWSCC. Moreover, the nozzle-specific Alloy-600 material exhibited additional atypical behavior through intergranular cracking in fatigue. The availability of measured CGRs for the actual Nozzle-3

material have allowed us to develop a more appropriate and realistic timeline for the growth of the long axial crack at Nozzle 3, which we have concluded occurred over a dramatically shorter time frame than previously considered.

These CGR data were clearly not available for the prior industry and plant specific predictive analyses performed in 1993, 1997 and 2001, prior to the 2002 Davis-Besse event. Further, these data were not available to the FENCO root cause investigation team or other analyses and investigations of the Davis-Besse event, such as those conducted by the NRC and the EPRI MRP since 2002.

Section 8.1 provides a brief background on PWSCC of Alloy 600 and stress analyses of CRDM nozzles performed prior to 2002 by industry groups. Section 8.2 presents the results of our stress analysis of Davis-Besse CRDM Nozzles 2 and 3. Section 8.3 reviews PWSCC CGR data used in previous industry analyses and data recently published in November 2006 by the NRC and ANL. is the ANL data are specific to the Davis-Besse CRDM nozzle and weld materials. In Section 8.4, the stress analysis results and the recently published CGR data are used to arrive at best estimates of when the cracks at Nozzles 2 and 3 first grew above the weld and began leaking and the rapid progression of cracking above the weld through to February 2002.

8.1 PWSCC and Prior Industry Stress Analysis Studies

8.1.1 PWSCC of Alloy 600 Materials in PWRs

Alloy 600 has been widely used in the PWR industry worldwide, and stress corrosion cracking problems first arose in the early 1970s in Alloy-600 steam-generator tubes, largely as a result of off specification secondary system water chemistry. However, in the early 1980s, cracking on the inside, or primary coolant side, of highly stressed areas of Alloy-600 steam-generator tubes was found to occur under chemistry conditions that had been carefully controlled. This cracking became known as primary-water stress corrosion cracking, or “PWSCC”.

The discovery of PWSCC in steam generator tubing was closely followed by its discovery in Alloy-600 pressurizer nozzles in CE plants at the highest operating temperature location in the primary coolant system of these PWR units, and in 1991, the first PWSCC of a CRDM nozzle was discovered at Bugey-3 in France.

The potential danger presented by reactor damage, however remote, has lead to an extensive effort has been expended over the last 30 years or so in investigating PWSCC of Alloy 600, with CRDM-nozzle cracking adding the latest chapter. There is an extensive body of published work on this subject, including the EPRI PWSCC workshops in 1991, 1992, 1994, 1997 and 2000 that are described in some detail in Section 5, along with relevant operating experience and the industry response to PWSCC of CRDM nozzles.

Stress corrosion cracking occurs when a susceptible material, under sufficient tensile stress, is exposed to a corrosive environment[1]. Alloy 600 has long been recognized as a material that is susceptible to stress corrosion cracking and also to PWSCC when subjected to high tensile stress in nuclear-reactor primary coolant.[2 3 4 5] Alloy-182 weld filler metal, which has a chemical composition similar to that of Alloy 600, also exhibits stress corrosion cracking under such conditions.[6]

Over the years, the industry and regulators learned that the key variables in the PWSCC process include microstructure, temperature, and the total tensile stress level. As in all SCC phenomena, the overall degradation process consists of crack initiation followed by crack propagation (growth). The temperature and especially the stress dependencies of the crack initiation and propagation processes are quite different. The stress dependence for PWSCC crack initiation involves stress (σ) raised to the fourth to fifth power (σ^4 to σ^5); whereas, the stress dependence of PWSCC crack propagation is almost linear.[a]

The high tensile stress that contributed to PWSCC cracking in the mill-annealed Alloy-600 CRDM nozzles and Alloy-182 J-groove welds at the Oconee and Davis-Besse plants was a combination of welding-induced residual stress from fabrication and operational stress produced by primary-coolant temperatures and pressures.

PWR operational stress at these plants was limited by design in compliance with the ASME Boiler and Pressure Vessel Code. These stress levels would not be expected to initiate PWSCC in the lifetime of the plant. However, in B&W reactor vessels like the one at Davis-Besse,

[a] Crack propagation (or growth) rate is a function of crack tip stress intensity factor or K (crack driving force), which, for example, in the EPRI/MRP crack growth rate (CGR) relation for Alloy-600 is raised to the power of 1.16, with the stress intensity factor itself being directly proportional to stress.

welding-induced residual stress can approach the yield strength of the material because the Code did not foresee the need for post-welding heat treatment for these weldments. Therefore, high stress poses an issue in virtually all CRDM penetrations in B&W-design PWRs because the J-groove welds were not required to be post-weld heat treated for stress relief.

Further, there can be interaction between the number of cracks, their size and shape, and the evolution of the crack front. The generally held view is that the overall degradation process is one where multiple small cracks first initiate with an initial shape approximating that of a semicircle or "half-penny". This event is then followed by the growth and linking-up of these cracks to form a single, much longer, semi-elliptical crack that has approximately the same depth as the coalescing cracks, and which then continues to rapidly propagate and grow in length and depth. During the crack propagation process the primary "driving" force for the process is the value if the crack-tip stress intensity factor, or "K". However, K is not only a function of crack length but also a strong function of crack shape. For the same local stress, the stress intensity factor for the long, semi-elliptical, linked-up crack, can be as much as two times that of the individual small semi-circular shaped cracks, with the result that an increase in K, and hence crack growth rate, of up to an order of magnitude can rapidly occur.

Ignoring this nonlinear aspect of early PWSCC crack development can lead to over-estimation of the time required to grow a crack, for example, through-wall in a nozzle. This results from the assumption that all of the growth occurs in a single crack, and that the time required for that crack to grow to its final observed length can be reliably estimated from the CGR versus K relationship for a single crack.

However, the reality that a single large PWSCC crack frequently results from the linking-up of multiple smaller cracks means that a number of small cracks can quickly link up or join to form one longer, rapidly-growing crack. Moreover, this single crack is actually larger in crack surface area than the combined crack surface areas of the smaller cracks. Thus, there can quickly be a sizable nonlinear increase in overall crack size as a result of very little PWSCC growth.

To illustrate this point, Figure 8.1 shows a laboratory-generated SCC crack in an Alloy-600 steam-generator tube (Figure 8.1(a)) as well as an actual steam-generator tube crack (Figure

8.1(b)) along with the eddy-current signal (Figure 8.1(c)) for the same crack during the previous operating cycle, before the crack penetrated the tube wall. The length of the actual steam-generator tubing crack was approximately four inches. For the cracks in Figure 8.1(a), the stress intensity factor K for the small cracks labeled A, B, C, and D) was approximately 4 to 5 ksi-$in^{1/2}$, while the stress intensity factor for the larger (wider) crack (labeled D) was approximately 12 to 15 ksi-$in^{1/2}$ for the same crack depth and loading. The regions labeled 2 and 3 denote non-SCC regions.

The combination and interdependence of the factors discussed above can lead to very fast crack growth. For this reason, the use of a straight linear assumption for the CGR - i.e., a single crack growing according to a laboratory-generated CGR relation - can lead to over estimating the overall crack growth time.

8.1.2 Prior Industry Stress Analysis Studies

A number of industry studies performed in the last decade and a half have included finite element stress analyses of CRDM nozzle penetrations in B&W-design PWRs. In a 1993 analysis, B&W conducted a stress analysis to evaluate PWSCC crack growth rates and leakage rates.[7] In 1994, EPRI released a report on a multi-year study that included development of a detailed finite element stress analysis by Dominion Engineering Inc. (DEI) for circumferential cracking in CRDM nozzles.[8] In 2002, after discovery of the head wastage at Davis-Besse, DEI enhanced their earlier EPRI analysis model with a refined mesh and updated material properties in a CRDM finite element analysis performed to evaluate axial PWSCC cracks and leak rates for FENOC.[9]

8.2 Stress Analysis of Davis-Besse CRDM Nozzles 2 and 3

This section describes the finite element stress analysis of Davis-Besse CRDM Nozzle 3 that we have performed for the purpose of evaluating residual and operational stress states and their effect on axial PWSCC cracks and leakage rates leading to formation of the observed wastage cavity. Analysis results confirm that: 1) tensile stresses in the CRDM nozzle and adjacent J-groove weld were of sufficient magnitude to cause rapid propagation of PWSCC cracks, 2) tensile stresses in the J-groove weld approached the yield strength of the material under

operating conditions, 3) the predicted location of high tensile stress is consistent with the observed location and orientation of PWSCC cracks, and 4) results from this analysis are consistent with reported results from similar numerical simulations performed by others.[10 11 12]

Sections 8.2.1 through 8.2.4 provide summary descriptions of the finite element model, material properties, loading conditions, and stress results from the analysis. Details of the analysis inputs, assumptions, and results are provided in Appendix A.

8.2.1 Finite Element Model of CRDM Nozzle 3 Head Penetration

Numerical simulation of stresses in and around the Davis-Besse CRDM Nozzle-3 head penetration was performed using the finite element method, a widely used and accepted method of performing structural analysis. Simply stated, the finite element method provides a means by which a relatively large and geometrically complex structure of unknown behavior can be readily analyzed as an equivalent assembly of smaller regularly shaped elements (finite elements) of known behavior. The CRDM nozzle analysis was performed using the MSC.Marc program,[13] a widely used commercial finite element analysis program for nonlinear structural analysis.

A three-dimensional (3-D) finite element model (Figure 8.2) of Davis-Besse CRDM Nozzle 3, with surrounding RPV head material and J-groove weld, was constructed based on dimensional information obtained from Babcock & Wilcox (B&W) fabrication drawings and quality control records (see Appendix A). The analysis model represents a segment of the RPV head surrounding Nozzle 3 and extends half the distance to adjacent nozzles in each direction. Spherically symmetric boundary conditions were applied on the truncated boundaries so that the modeled segment responds as if it is a part of a full hemispherical head.

Advantage was taken of a plane of geometrical symmetry passing through the nozzle centerline along a meridian of the hemispherical RPV head. This plane of symmetry allowed for simulation of the full nozzle using a model representing only half of the nozzle. Appropriate boundary conditions applied on the symmetry (or cut) plane cause the half-symmetry model to behave just like the full nozzle. This common modeling technique optimizes solution efficiency by avoiding redundant calculations.

Figure 8.3 shows a close-up view of the J-groove weld region of the finite element model. For this analysis, the Nozzle 3 J-groove weld was assumed to be comprised of thirteen weld beads or weld passes. Information on the exact number and layout of weld beads in the Nozzle-3 weld was not available. However, the assumed size and number of weld beads is consistent with common welding electrode sizes and is similar to the pattern of weld beads in an analysis performed for the NRC research program on CRDM integrity assessment.[14]

The Davis-Besse RPV head and CRDM nozzles were fabricated with interference fits between the nozzles and the head penetrations.[15] This means that the outer diameter (OD) of each nozzle was machined to be slightly larger than the diameter of the corresponding penetration in the head. During RPV head fabrication, the CRDM nozzles were likely cooled in liquid nitrogen to shrink them and allow insertion of the nozzles into the head penetrations. Upon warming back to room temperature, the nozzles expanded into contact with the head penetrations, thus locking them in position. Modeled dimensions of the RPV head penetration and CRDM nozzle diameters were matched to B&W fabrication quality control records for Davis-Besse Nozzle 3 to provide the same level of interference fit in the analysis. The nozzle and head portions of the model are separate components with a contact interface between them.

Most B&W reactor head CRDM penetrations were counter bored prior to nozzle insertion so that the height of the interference-fit zone would be uniform around each nozzle. However, the Davis-Besse head penetrations were fabricated without counter bores;[16] therefore, the current analysis model does not include counter bores.

8.2.2 Material Properties

The RPV head assembly is largely comprised of four different materials. The hemispherical head is a forging of ASME SA-533 Grade B Class 1 alloy steel with an inner-surface weld cladding of Type 308 stainless steel.[17] The CRDM nozzles that are the subject of this analysis were fabricated from mill-annealed Alloy 600 (Heat M3935), a nickel-based alloy. The J-groove welds that join the CRDM nozzles to the alloy steel head were fabricated using Alloy 182, a nickel-based weld filler metal.[18]

The current thermal-structural analysis required both mechanical and thermal material properties as inputs. Mechanical property inputs included elastic modulus, Poisson's ratio, yield

strength (or flow stress), density, and coefficient of thermal expansion. Thermal property inputs included thermal conductivity, specific heat, and emissivity. Temperature-dependence was included for all properties that vary with temperature. In most instances, temperature-dependent material property data was obtained from the 2001 ASME Boiler and Pressure Vessel Code, Section II, Part D.[19] Where actual material test results for yield strength of Davis-Besse materials were available, the temperature-dependent data from the ASME Code were scaled to match the actual material data at room temperature. Actual test data for yield and ultimate strength of the Nozzle-3 Alloy 600 and the 308-SS cladding were obtained from the detailed metallurgical report on the samples removed from and tested in the laboratory.[20] For the Alloy 182 weld metal, thermal properties and the temperature dependence of mechanical properties for Alloy 600 were used. Property data was checked for consistency with that used in similar analyses performed for EPRI and the NRC.[21] [22] [23] Details of material property inputs to the analysis are presented in Appendix A.

Previous residual stress analyses performed by DEI[24] and EMC2[25] for EPRI and the NRC, respectively, have indicated that inclusion of work hardening effects in the weld metal stress-strain relationship tends to over predict residual stresses from weld shrinkage. As was done in these earlier analyses, we modeled the constitutive behavior of the Alloy-182 weld metal as elastic-perfectly plastic to avoid this over prediction of stress. A work-hardening constitutive model for the Alloy-600 nozzle material, similar to the ones used by DEI and EMC2 was used in this analysis.

8.2.3 Loading Conditions

The stress state in and around a CRDM penetration J-groove weld is a combination of welding-induced residual stress and operational stress from primary coolant pressure and temperature. The residual stress is a result not only of weld shrinkage during cool down after welding, but also head stress relief after weld buttering and some localized plastic deformation during the pre-service hydrostatic pressure test. The analysis simulation included loading steps to simulate:

- application of weld buttering in the J-groove (with cooldown to room temperature), [26]

- buttering/head stress relief (1125°F[27]),
- nozzle shrink fit (nozzle cooled and expanded into head penetration), [28]
- sequential application of 13 J-groove weld passes (with cooldown to below 350°F[29] between passes),
- a hydrostatic pressure test to 3,125 psi,[30]
- operating pressure of 2,155 psi and operating temperature of 605°F (318°C).[31]

8.2.4 Stress Analysis Results

The numerical simulation was performed using a coupled, nonlinear, thermal-mechanical solution process wherein each analysis sub-step included a transient heat transfer solution followed by a thermal-mechanical stress solution. Incremental temperatures, displacements, stresses, and strains were stored for each step of the analysis. Only the relevant final operational stress results affecting PWSCC growth rates and crack opening are presented in this section. Detailed results at intermediate steps are presented in Appendix A.

The highest tensile stresses under full-load operational pressure (2,155 psi) and temperature (605°F) conditions occur in the J-groove weld. Figure 8.5 and Figure 8.6 are stress contour plots of circumferential (hoop) and axial stress around the J-groove weld on the downhill side (0°position) of Nozzle 3. Operational tensile hoop stress magnitudes in the J-groove weld range from roughly 30 to 110 ksi, with the majority of the weld in excess of 60 ksi. These high tensile stresses are largely due to weld thermal shrinkage during cool down after the welding process.

The nozzle wall adjacent to the weld gets pulled outward by the residual stress from weld shrinkage during fabrication and is pushed outward even more by coolant pressure during operation. Under full-load operation, hoop stress in the nozzle wall adjacent to the weld ranges from just over 20 ksi at the inside of the nozzle wall to well over 70 ksi at the weld line on the outside of the nozzle wall. These high stresses in both the weld and nozzle wall would be sufficient to initiate and propagate PWSCC cracks in both locations.

As shown in Figure 8.6, axial stress in the nozzle wall under full-load operating conditions is substantially lower than the hoop stress. A peak tensile axial stress of just less than 14 ksi occurs slightly above the top of the J-groove weld on the inside of the nozzle wall. This prediction of substantially lower axial stress than hoop stress is consistent with the observation of predominantly axial cracking in Davis-Besse Nozzles 2 and 3.

The analysis results confirm that: 1) tensile stresses in the CRDM nozzle and adjacent J-groove weld were of sufficient magnitude to cause rapid propagation of PWSCC cracks, 2) tensile stresses in the J-groove weld approached the yield strength of the material under operating conditions, 3) the predicted location of high tensile stress is consistent with the observed location and orientation of PWSCC cracks in Nozzle 3, and 4) results from this analysis are consistent with reported results from similar simulations performed for EPRI and the NRC.

8.3 PWSCC Crack Growth Rates for Davis-Besse CRDM Nozzles

Here we first briefly summarize in Section 8.3.1 the CGRs used in previous analyses of crack growth and consequential leakage, including those used in the FENOC root cause report as a key input into the timeline for the large wastage cavity at Nozzle 3.

In Section 8.3.2 we review the recently published (November 2006) data for CGRs of actual Davis-Besse Nozzle 3 Alloy 600 samples, as well as the CGR's for Alloy 182 weld material sampled from Davis-Besse Nozzle 11 weld.

8.3.1 Crack Growth Rates Used in Previous Work

The crack growth rate used in the 1993 B&W safety assessment (BAW-10190P) was "based on currently available industry data for Alloy 600 PWSCC."[32] The analysis used the Scott model which had been developed from PWSCC data for steam generator tubing, and the BAW-10190P report states that this model was "considered the most conservative model available for Alloy 600 PWSCC on SG tubing", and would be used "in the absence of PWSCC testing of prototypical Alloy 600 material used in the CRDM nozzle fabrication." [33]

The B&W analysis estimated the time required for a crack initiated on the wetted ID surface two inches above the weld to grow through-wall was six years, implying an average CGR of about 0.1 in/yr (0.62-in/6-yr). A through-wall axial crack was then calculated to grow from 0.5 inch to 2.0 inches in 4 years, and from 2 inches to 2.5 inches in a further 2 years, implying CGRs of 0.38 and 0.25 in/yr respectively.

The BAW-10190P report notes that the analysis was very conservative, and that even with the assumptions made, the crack would still be contained within the length of the RPV penetration.[34] We note that this analysis report, while it included a leakage and wastage assessment, was primarily focused on the safety aspects of a nozzle failure due to cracking.

The Davis-Besse CRDM susceptibility to cracking was evaluated in a ranking model developed by EPRI and used by B&W in the BAW-2301 report in 1977,[35] which was later submitted by FENOC in early 1999 to the NRC.[36] The ranking analysis used the Westinghouse plant at DC Cook-2, the only US plant at that time to have found a CRDM crack in a single nozzle, as the baseline cracking plant to respond to NRC GL 97-01.

The analysis did not assume a CGR explicitly, but effectively assumed that the Davis-Besse CRDM nozzles would exhibit the same CGR as D.C. Cook-2 had. The analysis placed Davis-Besse in the "moderate" susceptibility group, meaning that Davis-Besse was calculated to be likely to develop a CRDM nozzle crack similar to that found at DC Cook-2 in 5 to 15 EFPY of operation beginning on January 1, 1977. In contrast, the three Oconee plants were all placed in the "high" susceptibility group, being less than 5 EFPY away from developing a crack the size of the crack at DC Cook-2. In retrospect, this analysis was not correct for Davis-Besse, since the extensive cracking in Nozzle 2 and the large crack in Nozzle 3 developed in less than 5 EFPY.

Similarly, subsequent to the extensive cracking discovered in the Oconee-3 CRDM nozzles in February 2001, assessments were made by the EPRI MRP of the relative susceptibility of the Davis-Besse plant to CRDM nozzle cracking as compared with Oconee-3. These analyses did not assume a CGR explicitly, but again effectively assumed that the Davis-Besse CRDM nozzles would exhibit the same CGR as Oconee-3 had.

It was that key assumption that led to the prediction in the MRP-48 report (August 2001) that, as of March 2001, Davis-Besse was 3.1 EFPY away from experiencing cracking to a similar extent as Oconee-3.[37] That assessment was clearly optimistic, because the Davis-Besse Nozzles 2 and 3 were found in February 2001 to have extensive cracking and a long axial crack respectively, in less than 1 EFPY from March 2001. Just from the actual Davis-Besse Nozzle 2 and 3 experience, it is evident that the Davis-Besse CGRs were in fact higher than those at Oconee-3, which had the same M3935 heat of Alloy 600 material in 68 out of 69 CRDM nozzles.

Finally, the CGR assumed in the FENOC root cause report for crack growth from initiation to through wall, and from through wall above the weld to the final crack length measured in February 2002, was 4 mm (0.16 inches) per year[38]. This CGR was in line with the earlier CGRs assumed in the B&W (1993 and 1997) and EPRI MRP (2001) that we discussed above.

8.3.2 Recent Data on Davis-Besse Nozzle and Weld Alloy 600/182 Materials by NRC/ANL

PWSCC growth rate testing has been recently performed at Argonne National Laboratories on samples of Alloy 600 specifically taken from Davis-Besse CRDM Nozzle 3 and Alloy 182 taken from Davis-Besse CRDM Nozzle-11 J-groove weld.[39] These tests were performed at 600°F in simulated PWR primary water containing 2 ppm lithium, 1000 ppm boron, roughly 2 ppm dissolved hydrogen (about 23 cm^3/kg), and less than 10 ppb dissolved oxygen. Both half-thickness (1/2T) and quarter-thickness (1/4T) compact-tension (CT) specimens were tested. The 1/4T specimens consistently exhibited lower growth rates than did the 1/2T specimens, indicating a trend toward higher growth rates in conditions of greater triaxial constraint. In-situ cracking in a CRDM nozzle or J-groove weld would provide even greater triaxial constraint than a 1/2T test specimen.

Constant-load crack growth rate results for the Davis-Besse Nozzle 3 Alloy 600 are plotted in Figure 8.4 along with the EPRI/MRP disposition curve proposed for evaluation of CRDM integrity. Also plotted is a curve fit to the Nozzle 3 Alloy-600 data points using the EPRI/MRP crack growth rate function. The crack growth rates represented by the curve fit to the Davis-Besse Nozzle-3 material are three times faster than the EPRI/MRP disposition curve for Alloy 600, which itself represents the 75th percentile fit to 26 sets of Alloy-600 PWSCC growth rate

data. Further, the curve fit to the Davis-Besse Nozzle-3 material lie at approximately the 95th percentile for the 26 sets of Alloy-600 PWSCC growth rate data in the EPRI/MRP database. The fastest growth rate obtained for the Davis-Besse Nozzle-3 Alloy 600, which was 0.32 inches per year, is nearly four times faster than the rate predicted by the EPRI/MRP disposition curve for the same stress intensity factor, or crack driving force, K.

The implications of these results are important to our understanding of how the crack and the leakage from it developed over time. First, it is evident that the long axial crack in Davis-Besse CRDM Nozzle 3 grew much faster than had previous been analyzed. This means that the point in time at which this crack – which was ultimately responsible for the large wastage cavity at Nozzle 3 – first went through wall above the weld was much later than the 1994 to 1996 time period previously assumed. This in turn leads to the conclusion that the six to eight year time period during which Nozzle-3 crack leakage was previously assumed to be present is too long by a factor of at least two.

These results for Davis-Besse Nozzle 3 material were unexpected. As the ANL researchers noted in the Executive Summary of their November 2006 report:[40]

> "The Davis–Besse nozzle alloy showed significant environmental enhancement of fatigue CGRs, and the SCC growth rates (i.e., CGRs under constant load) were a factor of 4–8 higher than those of the median curve for Alloy 600. These rates correspond to the ≈95th percentile values of the population; i.e., the nozzle material exhibits very high susceptibility to SCC compared to other heats of Alloy 600.
>
> A unique feature of the nozzle alloy is that it exhibits a predominantly intergranular fracture even during fatigue loading. Transgranular growth is observed at the very beginning of the test (i.e., near the machine notch), but, in most cases, the crack becomes intergranular when the first grain boundary is encountered. The fact that intergranular growth takes place in a regime dominated by mechanical fatigue (which normally results in transgranular growth) suggests that the grain boundaries must have suffered some form of sensitization either during fabrication and/or during two decades in service.

> The reason for the high growth rates for the nozzle alloy is not clear. Metallographic examination of the Davis–Besse CRDM Nozzle #3 Alloy 600 revealed a "good" microstructure, i.e., extensive grain– boundary coverage of Cr–rich carbides, and relatively low or average tensile strength. These conditions are typically associated with low susceptibility of the material to PWSCC. Differences in the microstructure in terms of extent and nature of carbide precipitation may be important."

We note here that the "susceptibility rankings" developed by both B&W and the EPRI MRP in the 1993 to 2001 time frame, discussed in detail in Sections 5.3 of this report (and in 8.3.1 above), were likely the best estimates that could have been made at the time, absent specific data from a specific nozzle such as that reported by ANL in 2006. As noted in the citation from the ANL report above, the Davis-Besse Nozzle-3 Alloy-600 material exhibited a "good" microstructure, as indicated by metallurgical properties such as "extensive grain boundary coverage by Cr-rich carbides and relatively low or average tensile strength", properties typically associated with "low susceptibility" to PWSCC.

These were the properties used in the relative Alloy-600 susceptibility rankings, and were especially applicable to the EPRI MRP ranking of Davis-Besse in MRP-48 in August 2001 (Section 5.3.6). That ranking used Oconee-3 as its base plant, and Oconee-3 used Alloy-600 heat M3935 for 68 of its 69 CRDM nozzles. Nozzles 1 through 5 at Davis-Besse were also made from Alloy-600 Heat M3935, and so the 3.1 EFPY projected for Davis-Besse to experience cracking to the extent found at Oconee-3 in February 2001 was especially applicable to these five Davis-Besse nozzles. The ANL data for the Nozzle 3 Alloy-600 material shed light on why that 3.1 EFPY projection proved to be incorrect.

Figure 8.9 shows a similar plot of the PWSCC growth rate test results for the Alloy-182 weld metal taken from the J-groove weld of Davis-Besse CRDM Nozzle 11. These results indicate the Nozzle 11 weld metal exhibited growth rates lower than those represented by the EPRI/MRP disposition curve for Alloy 182. It should be noted, however, that the variability of PWSCC growth rates in weld metal is substantially greater than that of wrought material, such as Alloy 600.

We note that these new data were not available to the FENOC root cause investigation team since they were only recently published in November 2006. However, as we discuss in Sections 8.4.3 and 8.4.4, these recent test data are highly relevant to the timeline progression of events at Nozzle 3, since the CGR used in the FENOC root cause investigation (0.16 inches per year) was only around half of these recently measured rates.

8.4 PWSCC Cracks in Davis-Besse CRDM Nozzles 2 and 3

This section characterizes the size and shape of the large PWSCC cracks in Nozzles 2 and 3, and explains why previous interpretations of leak size based on crack length above the weld are incorrect. Section 8.4.1, explains how we arrived at what we have called the "effective crack length for leakage" for the cracks at CRDM Nozzles 2 and 3, which is not the same as the crack length measured and reported in the Framatome UT inspection report. Section 8.4.2 presents a composite schematic of the large crack in the nozzle wall and weld of CRDM Nozzle 3 that was developed using both the Framatome UT inspection data[41] and the BWXT metallurgical examination results[42] from the removed section of RPV head and weld.

8.4.1 Effective Crack Lengths for Leakage in Nozzles 2 and 3

The effective crack lengths for leakage created by the axial PWSCC cracks in Davis-Besse Nozzles 2 and 3 were actually less than indicated in the Root Cause Report[43] based on ultrasonic testing (UT) results from Framatome examinations[44] of the nozzles at 13RFO and subsequent UT crack profile data analysis by Framatome.[45] The source of this discrepancy stems from the fact that the Framatome UT reports tabulated and plotted the axial extent of the cracks based on the locations of the extreme crack tips, which does not account for the through-nozzle-wall extent of the cracks near the tips. In many instances, the axial PWSCC crack tips extended well above the level of complete through-wall cracking.

An excellent example of this can be seen in Crack 8 of Nozzle 2. Figure 8.7 is a plot excerpted from the Framatome UT report[46] showing the extent of PWSCC cracks in CRDM Nozzle 2 based on UT data. This figure effectively represents an unrolled 360° view of the inside of Nozzle 2 showing the size and location of all PWSCC cracks identified by the Framatome UT inspection. The two undulating horizontal lines indicate the location of top and bottom of the J-

groove weld on the outside of the nozzle, and the vertically oriented, angled lines crossing the J-groove weld indicate the location and extent of the nine axial PWSCC cracks in Nozzle 2. Axial Crack 8, the second from the right in the figure, is shown to extend 1.15 inches above the top of the weld, suggesting a sizable leak path. However, a more detailed examination of the UT results, including the through-wall profile of the crack, as shown in Figure 8.8, revealed that the actual effective crack length for leakage (marked by blue arrows) is considerably smaller, only about 0.24 inch between the tip of the weld and the closest approach of the crack front (the edge of the black region representing the crack).

Through similar detailed geometrical analysis of the Framatome UT data for all axial PWSCC cracks in Nozzles 2 and 3, we calculated the limiting effective crack length for leakage for all cracks extending above the top of the J-groove welds in these two nozzles. Appendix B summarizes the results of these calculations for Nozzles 2 and 3, respectively. These results clearly show that Crack 1 in Nozzle 3, the crack associated with the large wastage cavity, had by far the largest effective crack length for leakage of any of the axial cracks in the two nozzles.

8.4.2 Reconstruction of the Crack-1 Profile in CRDM Nozzle 3 and J-groove Weld

During the initial boring process to repair Davis-Besse Nozzle 3, which led to discovery of the wastage cavity, the majority of the large, leaking, axial PWSCC crack (Crack 1) on the downhill side of the nozzle was machined away. Only that portion of the crack that was left in the remainder of the J-groove weld was available for metallurgical examination. FENOC contracted with BWXT Services to perform metallurgical and fractographic examinations on the remaining pieces of the RPV head and J-groove weld surrounding Nozzle 3.[47]

We used ultrasonic testing data (see Figure 8.10) from the Framatome examination of CRDM Nozzle 3 during 13RFO[48] and photographs (see Figure 8.11) from BWXT metallurgical sectioning[49] of the remnant J-groove weld to compile a schematic of the final size and shape of the Crack 1 in Nozzle 3, as shown in Figure 8.12. Key points along the crack front are identified by red dots in the figure and labeled with the data source. Additional labels in the figure beginning with "A2A6…" identify the corresponding BWXT metallurgical samples.

It is clear from the schematic in Figure 8.12 that Crack 1 in Nozzle 3 not only breached the nozzle wall for an axial length of roughly four inches, including more than one inch above the J-groove weld, but also cracked through roughly two-thirds of the J-groove weld itself. This indicates that by the time the wastage cavity progressed down below the top of the J-groove weld, the size of the minimum leak path width included both the effective length of crack in the nozzle wall above the weld and the length of the crack on the outside of the J-groove weld. Thus, the flow-limiting width of Crack 1 in Nozzle 3 increased dramatically during development of the wastage cavity as the backside of the J-groove weld became exposed due to loss of the surrounding head steel.

8.5 Crack Growth Rates for Observed Cracks at Davis-Besse CRDM Nozzles 2 and 3

Here we apply the CGRs derived from the recent NRC/ANL CRG data for CRDM Nozzle 3 material, in conjunction with the stress analysis results for Davis-Besse Nozzle 3, to arrive at the probable times that the cracks observed in February 2002 originally reached through wall, and correspondingly how long it took those cracks to grow to the final length measured in February 2002.

8.5.1 Estimate of Time at Which Cracks in CRDM Nozzles 2 and 3 Reached Through Wall above Weld and Leakage Began

The FENOC Root Cause Report presented a scenario in which the longest crack in CRDM Nozzle 3 (Crack 1) reached the top of weld and began leaking in the 1994 to 1996 time frame, based primarily on observations of plant unidentified leakage, containment air cooler plugging, and radiation monitor filter plugging. Other investigations into the event, such as those conducted by the NRC, reached the same conclusion.

The FENOC Root Cause Report used a CGR of 4 mm per year (0.16 inches per year) to back-calculate the initiation of Crack 1 in Nozzle 3 in 1990 (+/- 3 years), based on the conclusion that the crack reached through wall and leakage began in the 1994 to 1996 time frame. For the longest CRDM Nozzle 3 crack to grow from the top of the weld in 1995 +/- 1 year to the final measured length at 1.2 inches above the weld in February 2002 implies a similar CGR. Based on our analysis and recent work done by Argonne National Laboratory, the CGR used by

FENOC was too low, and the actual times for through-wall cracking and growth above the weld were substantially shorter.

We estimated the level of crack driving force (crack tip stress intensity factor, K) for part-through-wall and through-wall cracks in Nozzle 3 using fracture-mechanics weight-function solutions in the NASCRAC™ Software and stresses from the finite element analysis. Under the high tensile hoop stresses in the J-groove weld and adjacent nozzle wall, described above in Section 8.2.4, the crack driving force estimated for the upper tip of Crack 1 in Nozzle 3 as it grew past the top of the J-groove weld was in excess of 50 ksi-in$^{1/2}$. Since hoop stress in the nozzle wall decreases above the top of the weld, subsequent growth of the crack above the weld exhibited decreasing crack driving force, but it was estimated to be at least 24 ksi-in$^{1/2}$ in the late stages of growth approaching February 2002.

The CGR data for Davis-Besse Nozzle 3, shown in Figure 8.4, indicates that at a crack driving force of 50 ksi-in$^{1/2}$, the CGR for the nozzle crack would have been about 0.8 inch per year, and about a quarter-inch per year at 24 ksi-in$^{1/2}$. Crack growth rates were interpolated based on K as a function of crack length above the weld and then integrated to obtain estimates of time to grow a long axial crack to various heights above the top of the weld. Details of this calculation are presented in Appendix B. Figure 8.13 shows the calculated time to grow the upper tip of a long axial crack in the nozzle and weld to various heights above the top of the weld. Based on these results, we conclude that the long through-wall crack discovered on the downhill side of Nozzle 3 in 2002 likely just reached above the top of the weld some time in the middle of Cycle 12, in mid-1999. At the calculated growth rates, the crack then reached the measured point, 1.2 inches above the weld, by February 2002.

By the time of 12RFO in April-May 2000, the upper tip of this growing crack would have been approximately 0.6 inch above the weld on the nozzle OD, with an effective crack length for leakage of slightly less than half an inch above the weld. For this effective crack length for leakage, the leak rate was miniscule, comparable to that observed at Oconee-1 for similar length cracks in November 2000.

The longest cracks based on effective length for leakage in CRDM Nozzle 2 measured 0.76 to 0.82 inch above the weld in February 2002. Assuming similar growth rates in Nozzle 2, these

cracks would have been below the top of the weld in April-May 2000 at 12RFO, and thus not leaking.

The analysis discussed above for the growth rate of part-through-wall and through-wall cracks in the nozzle wall also provided estimates of the level of crack driving force for the same cracks as they grew into the J-groove weld region at Nozzle 3. As described in Section 8.2.4, the tensile hoop stresses in the J-groove weld itself are higher than in the adjacent nozzle wall. The crack driving forces estimated for the J-groove weld region for the cracks considered ranged from 46 to 53 ksi-in$^{1/2}$, with corresponding CGRs of 0.67 to 0.96 inches per year.

Based on the substantially higher predicted crack driving forces in the weld and the UT profiles of the axial cracks in both Nozzles 2 and 3, we conclude that Crack 1 in Nozzle 3 grew more rapidly in the J-groove weld than in the nozzle wall. Further, Crack 1 likely initiated in or close to the OD of the nozzle at the bottom of the J-groove weld and grew rapidly upward through the weld and radially inward through the nozzle wall. Crack 1 ultimately grew far enough inward through the nozzle wall to either link up with ID-initiated PWSCC cracks or break through to the ID. The upward growth of Crack 1 through the J-groove weld progressed through the buttering layer near the top of the weld and continued upward into the nozzle wall as a through-wall crack.

By the time the J-groove weld crack was uncovered by the downward growing wastage cavity in October-November 2001 (see Section 10), we conclude that this weld crack had grown through the weld to a point close to its final observed size on the outside of the weld buttering in February 2002 (Figure 8.12). For CRDM Nozzle 2, the longest axial cracks had measured 0.76 to 0.82 inch above the weld in February 2002. Again using an average CGR of roughly a third of an inch per year, these cracks would have been about a quarter-inch above the weld in April-May 2000 at 12RFO. Cracks with such a small effective crack length for leakage, if they leaked at all, leaked at such a low rate that it would not have been detectable.

8.5.2 The Unique Nature of the Cracking in Nozzle 3

Crack growth rates (CGRs) in Alloy 600 (nozzles) and Alloy 182 (welds) can be highly variable and unpredictable. The general scatter in CGR data for both Alloy 600 and 182 is of the order of two orders of magnitude, or a factor of 100. This variability in CGR is self evident from the cracking behavior of CRDM Nozzles 2, 3, 4, and 5 at Davis-Besse, all of which were located in the same geometric position on the RPV head, all of which were fabricated from the same heat of Alloy 600, and all of which experienced essentially the same operational temperature and pressure history.

All four of these nozzles were manufactured by the same vendor, from the same heat of Alloy 600, using the same manufacturing processes, and were installed in the same geometric position on the RPV head by the same manual welding process. Yet Nozzle 4 exhibited no cracking, Nozzle 5 was found to have only one very short non-through-wall crack, Nozzle 2 had seven axial cracks (six of which were through wall) plus one circumferential crack, and Nozzle 3 had two through-wall axial cracks, one of which was the longest axial crack ever found in a CRDM nozzle.

Similar variations in cracking performance of apparently identical Alloy-600 CRDM nozzles at other PWR plants show that the process is highly variable. For example, at Oconee-3, 68 of the 69 CRDM nozzles were manufactured from the same M3935 heat of Alloy 600 as Davis-Besse Nozzles 1 through 5, yet only 14 of these nozzles experienced cracking, and only four experienced circumferential cracking. Of the five center CRDM nozzles at Oconee-3, only Nozzles 2 and 3 experienced cracking[50].

The same is true for cracking of the Alloy-182 welds, with one of the best examples being the weld cracking at the Westinghouse plants at North Anna-1 and North Anna-2. The RPVs for these units were manufactured by the same fabrication shop (Rotterdam Dockyard). At North Anna-1, only six out of 65 CRDM nozzles experienced weld cracks, while at North Anna-2, 42 of the 65 nozzles experienced weld cracks, the highest incidence of CRDM-weld cracking at any plant worldwide[51].

We attribute this variable performance to the manual welding process which can result in highly variable residual stress levels from nozzle to nozzle. Further, we have noted differences in

operating temperatures for the two hot legs at Davis-Besse, and since head temperatures are not measured, we do not know if the center nozzles such as Nozzle 3 were subjected to a higher fluid temperature than others.

Data on crack initiation and growth for both Alloy 600 and Alloy-82 weld metal indicate that the PWSCC process is generally one of initiation of multiple cracks followed by a growth and linkup process as multiple small cracks grow into each other and coalesce to form larger cracks. Analysis of the effect of this process, as well as observations in the field, indicate that rapid increases in crack growth can occur when several small cracks, growing relatively slowly, link up to form a larger crack with the same depth. Such linkup produces a relatively rapid rise in the crack driving force of the "linked" crack and can result in an order of magnitude or more increase in crack growth rate over a very short time period.

It is clear that the long axial crack in Davis-Besse CRDM Nozzle 3 was unique. The Nozzle-3 Alloy 600 itself exhibited extremely high crack growth rates, higher than those at CRDM Nozzles 2, 5 or 4. The long crack at CRDM Nozzle 3 was unexpected, unanticipated, and not predicted prior to 2002 by any industry-generic or Davis-Besse plant-specific work.

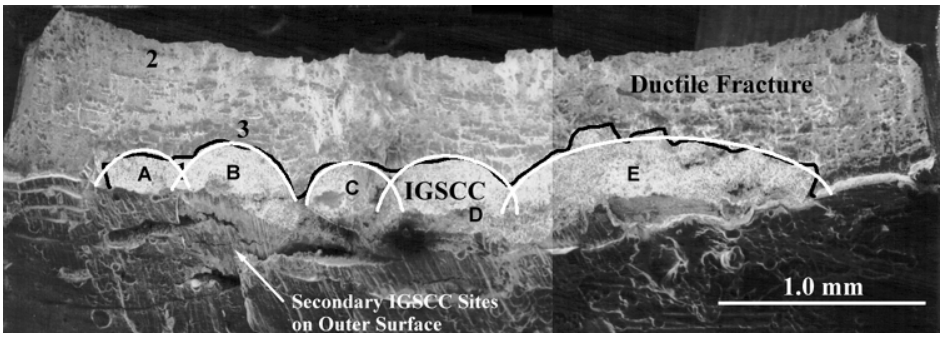

(a)

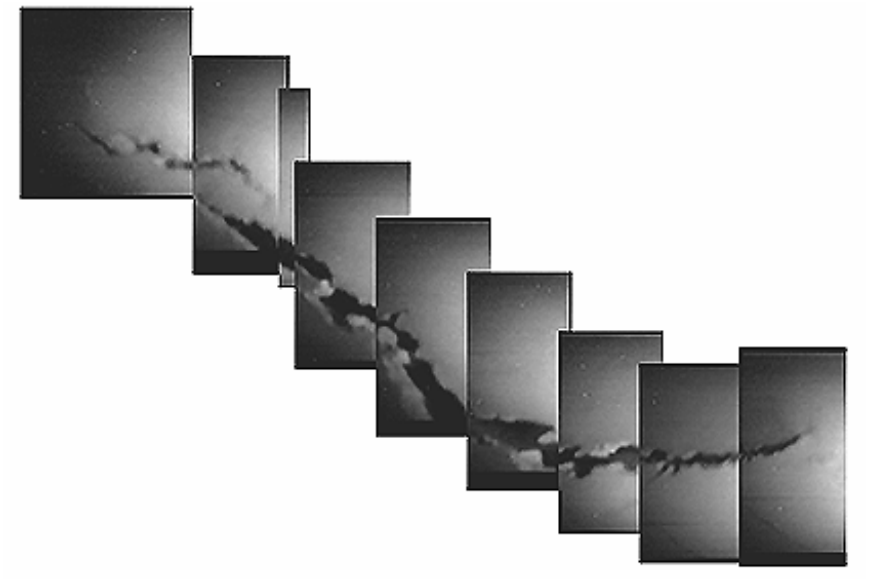

(b)

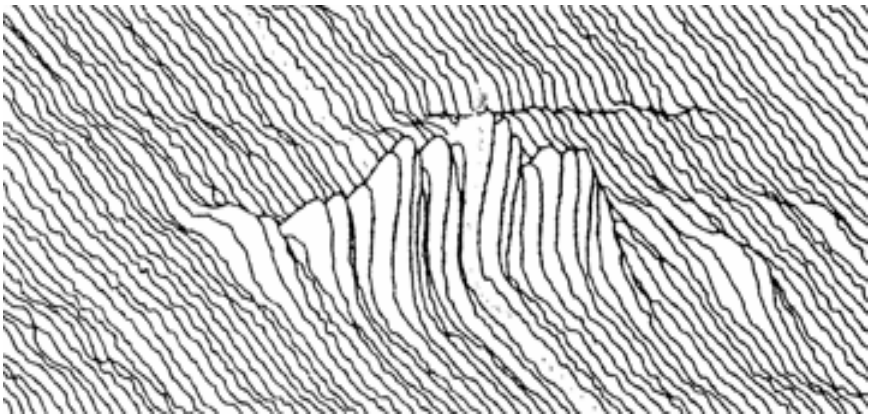

(c)

Figure 8.1 Crack initiation and growth in steam generator tubes, (a) lab-generated SCC cracks showing multiple crack initiation; (b) actual steam generator tube crack; (c) eddy current inspection signal from the tube crack in (b) one cycle earlier

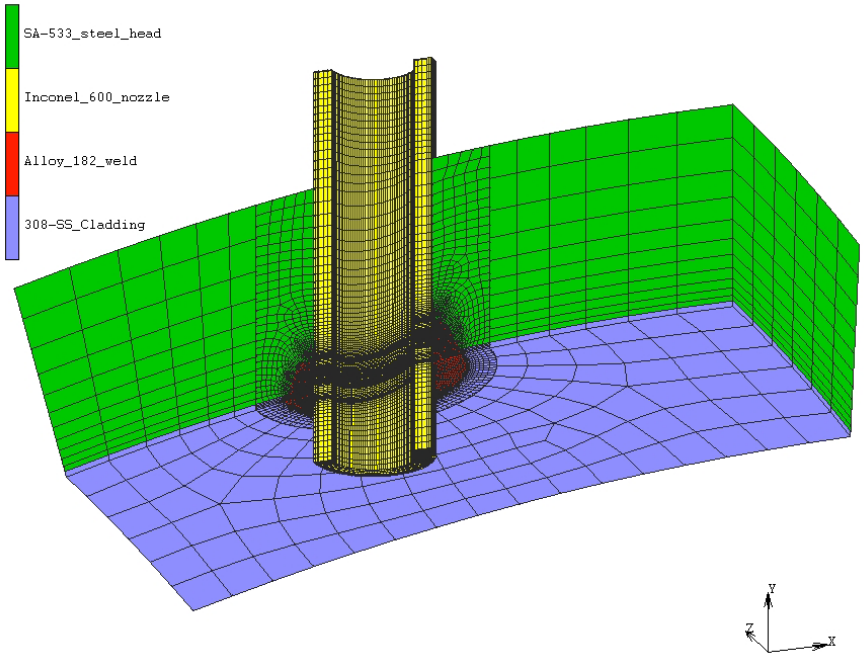

Figure 8.2 Three-dimensional, half-symmetry finite element model of CRDM Nozzle 3 head penetration, showing Alloy-600 nozzle, Alloy-182 J-groove weld, and surrounding SA-533 alloy steel head with Type 308 stainless steel cladding.

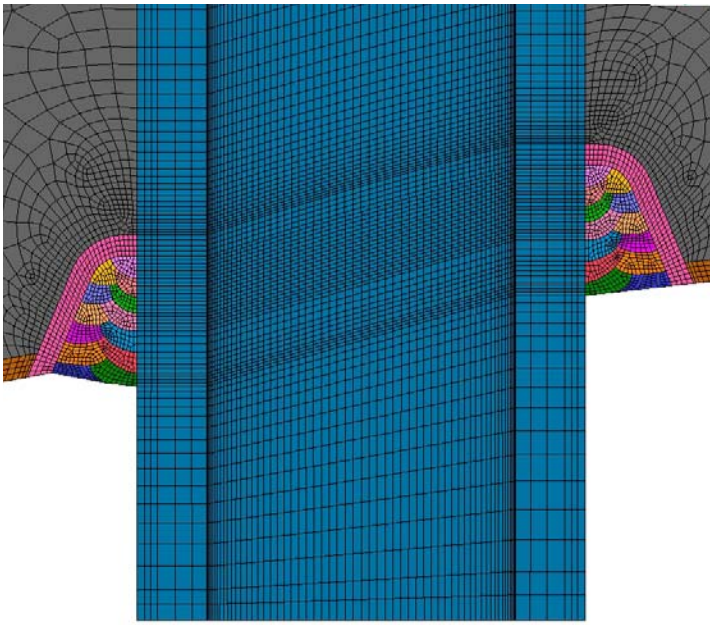

Figure 8.3 Close-up view of 13-pass J-groove weld joining CRDM Nozzle 3 to alloy-steel head.

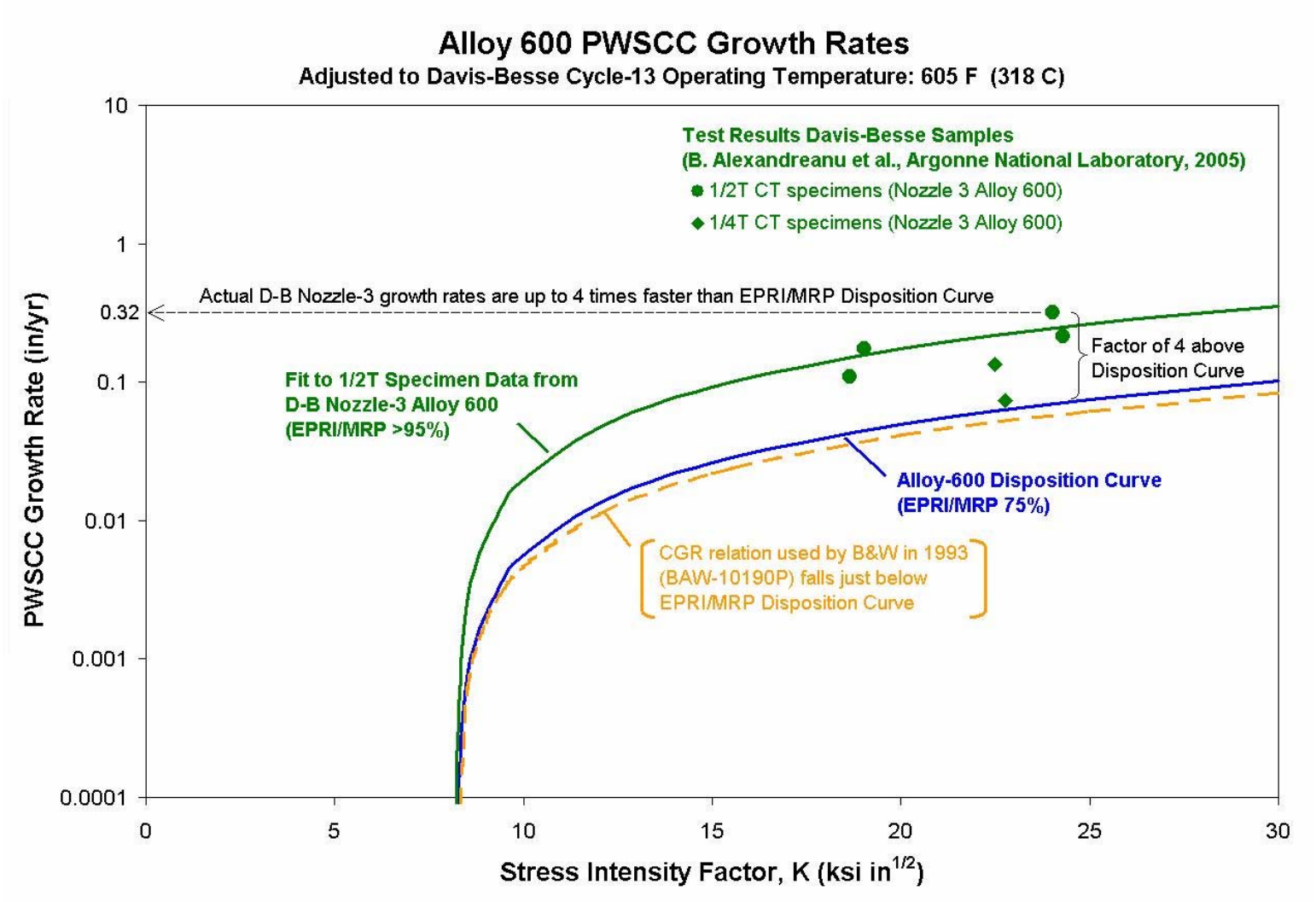

Figure 8.4 PWSCC growth rate data for Alloy 600 from Davis-Besse Nozzle 3 compared to EPRI/MRP disposition curve.

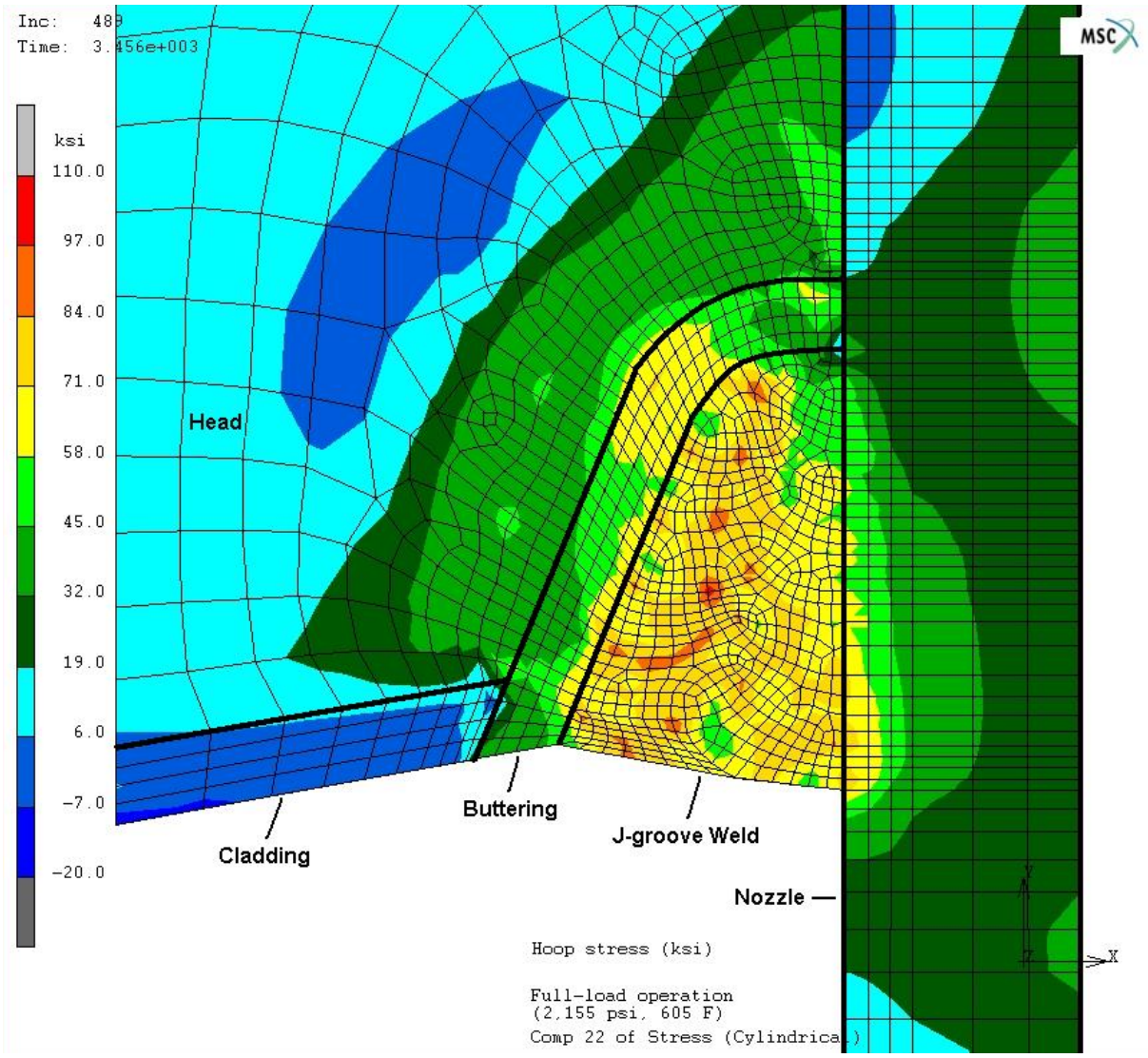

Figure 8.5 Nozzle-circumferential (hoop) stress results in ksi for downhill side of Nozzle 3 at J-groove weld under operating pressure and temperature (2,155 psi, 605°F).

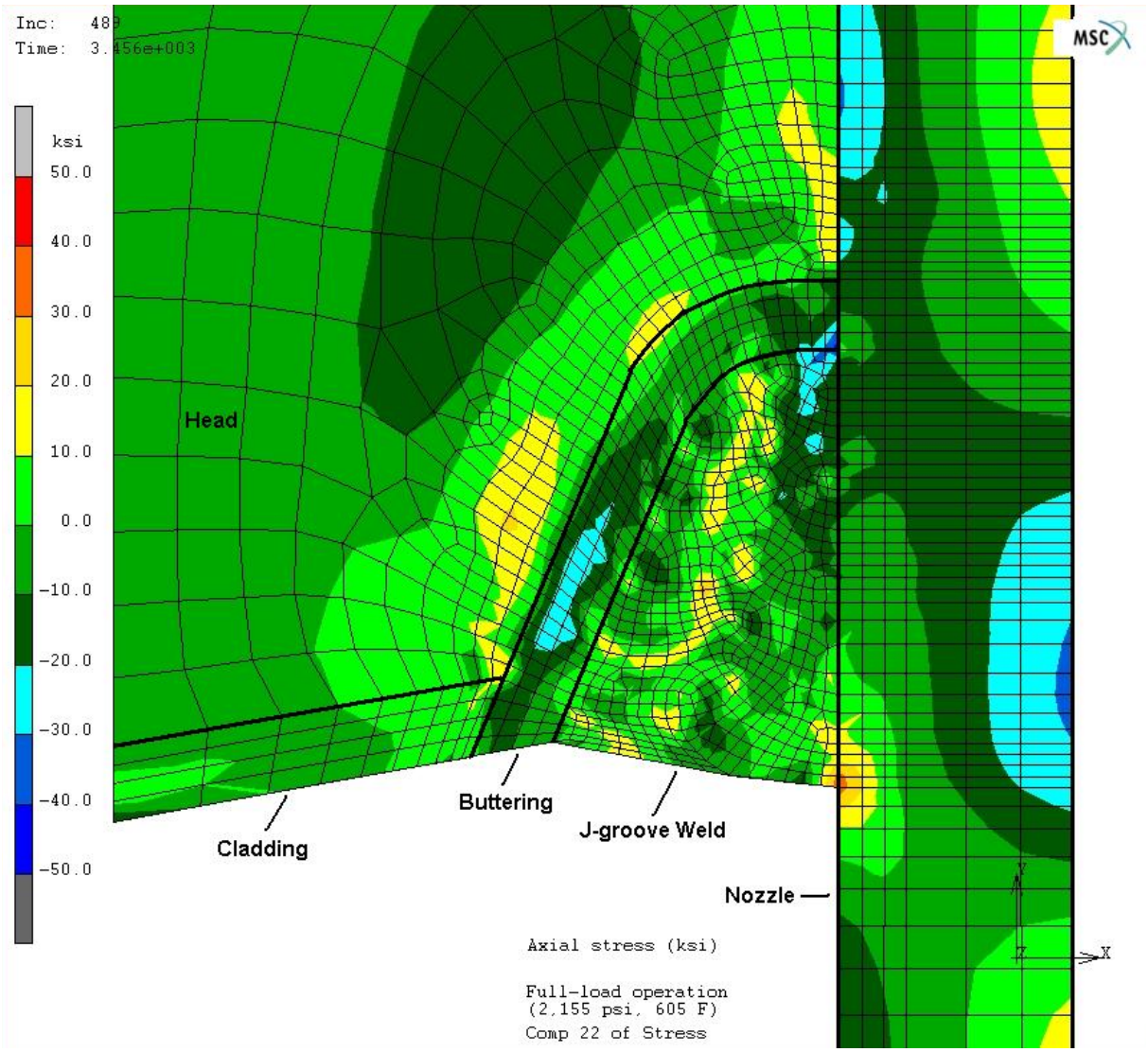

Figure 8.6 Nozzle-axial stress results in ksi for downhill side of Nozzle 3 at J-groove weld under operating pressure and temperature (2,155 psi, 605°F).

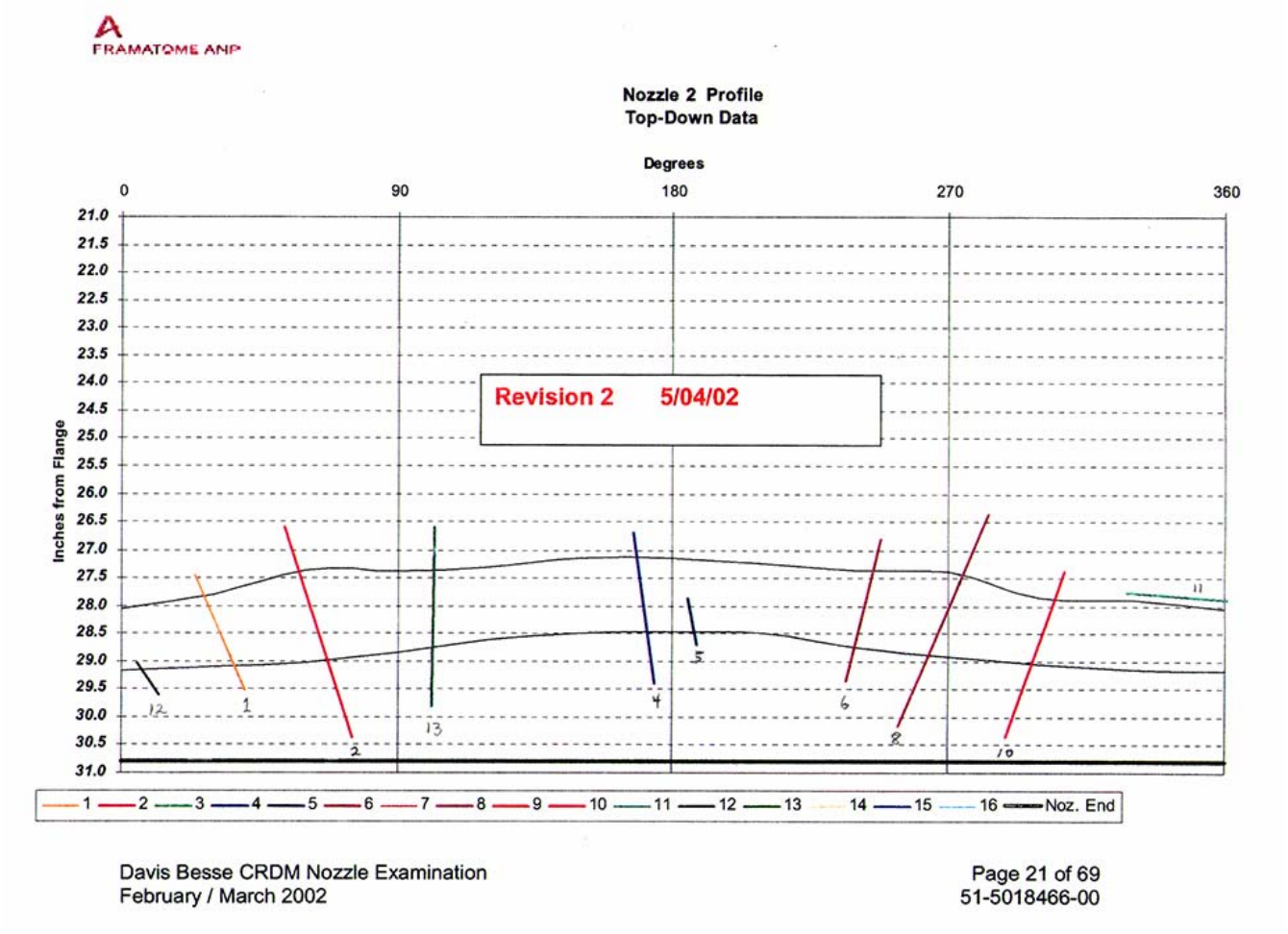

Figure 8.7 Framatome plot of crack profiles in Davis-Besse CRDM Nozzle 2 based on UT results. [Excerpted from Reference 44, with handwritten crack numbers added.]

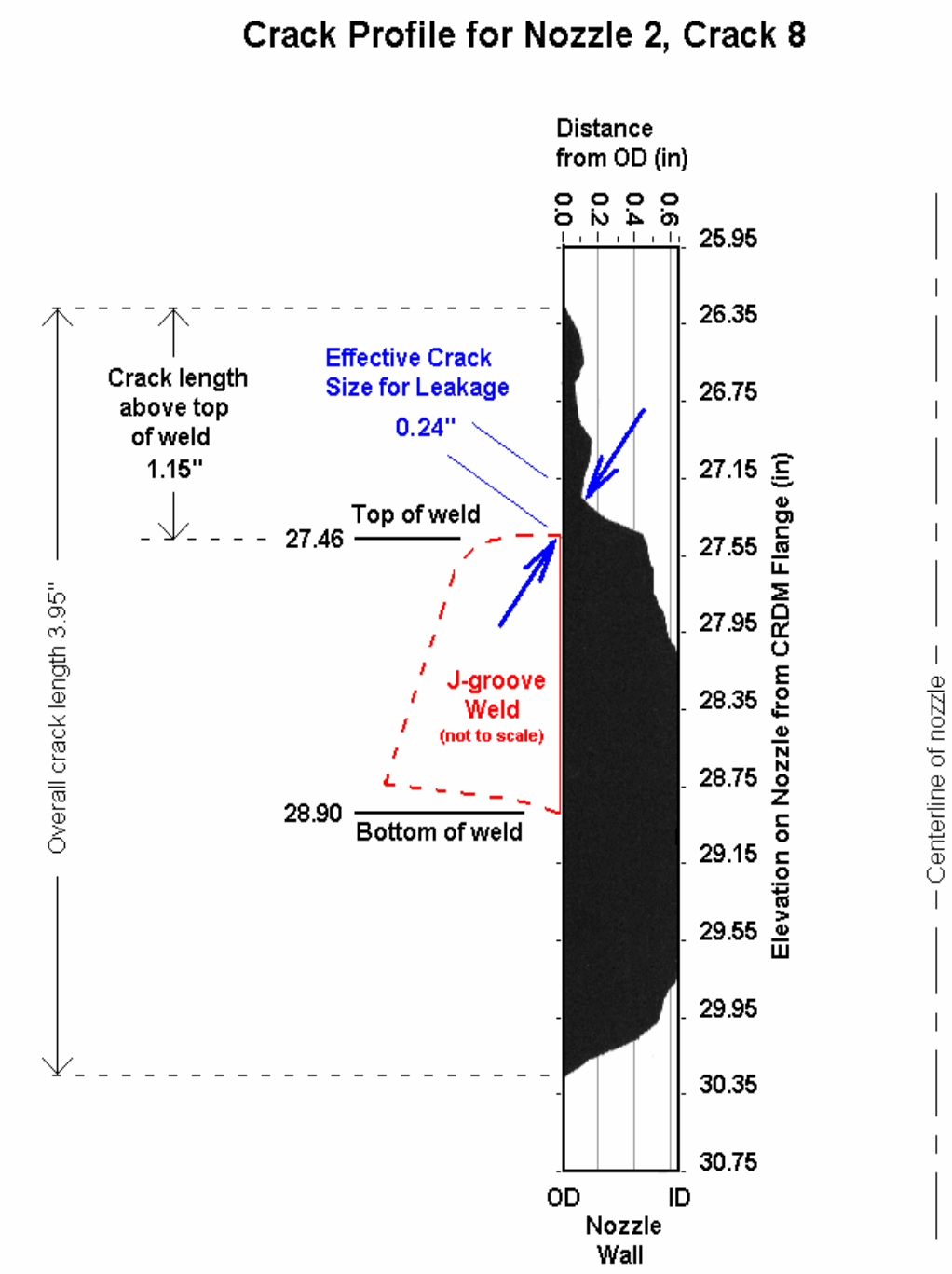

Figure 8.8 Through-wall profile of Crack in Davis-Besse CRDM Nozzle 2 based on Framatome UT results. [Adapted from Reference 45, with annotations added.]

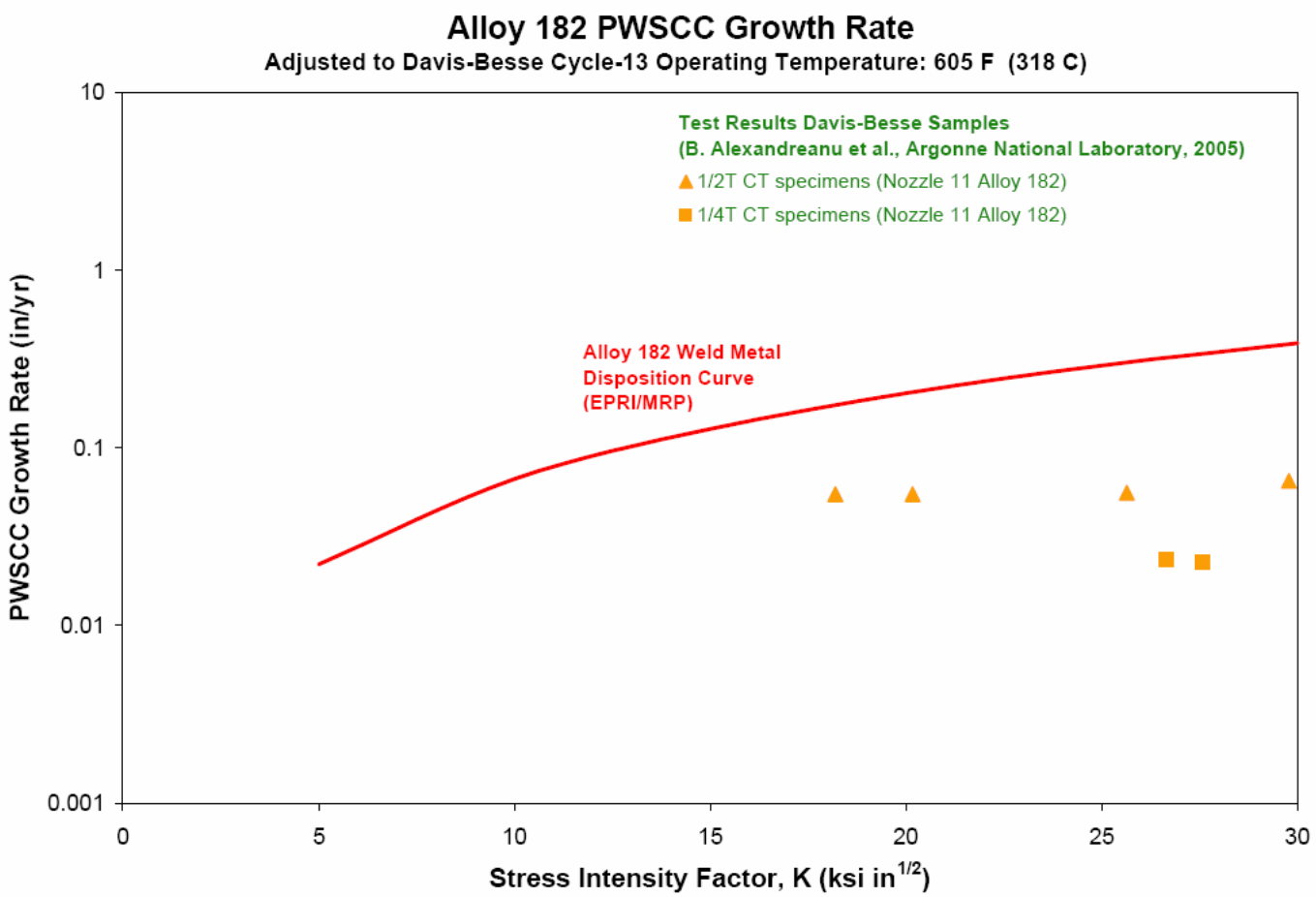

Figure 8.9 PWSCC growth rate data for Alloy 182 from Davis-Besse Nozzle 11 J-groove weld compared to EPRI/MRP disposition curve.

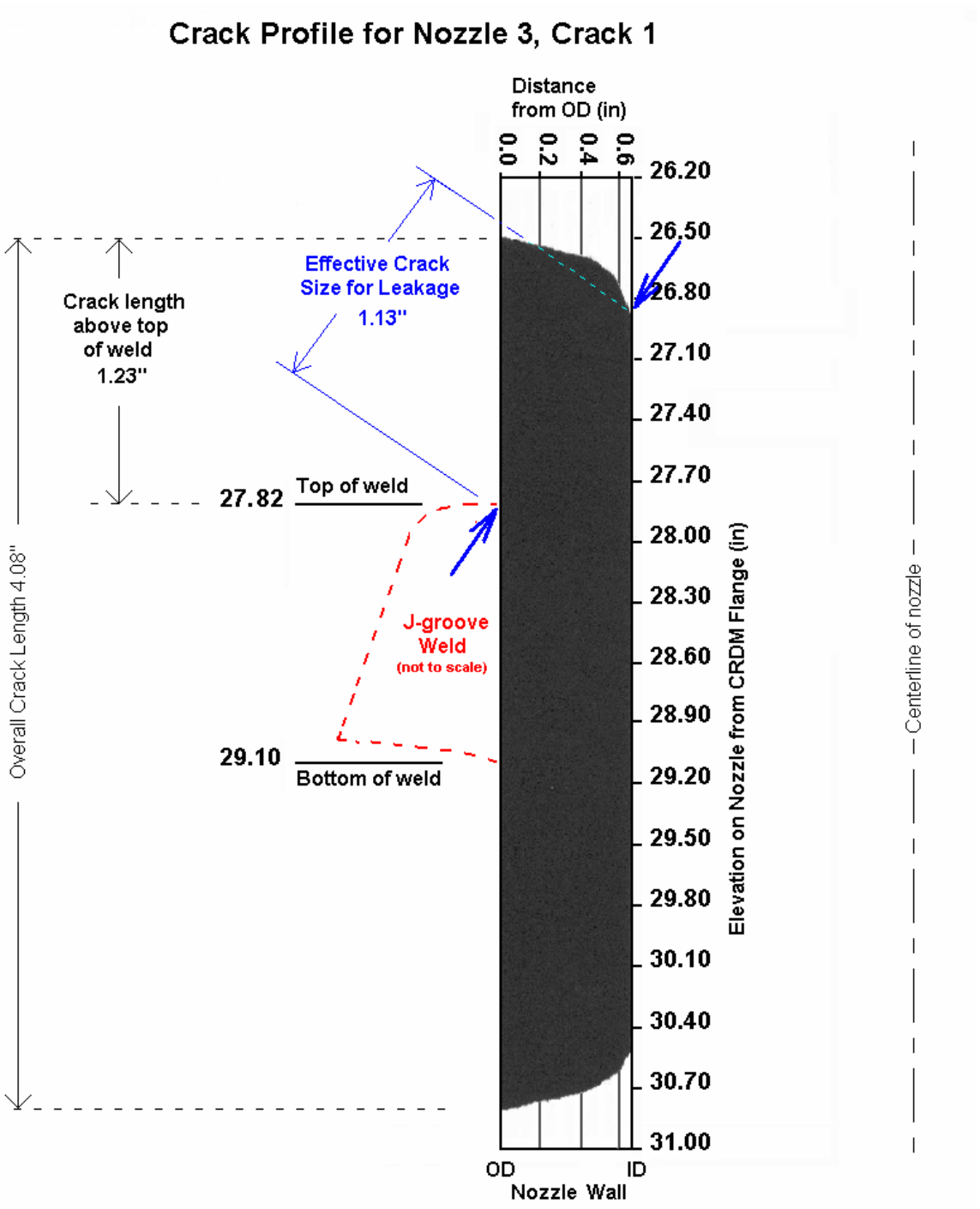

Figure 8.10 Through-wall profile of Crack in Davis-Besse CRDM Nozzle 2 based on Framatome UT results. [Adapted from Reference 45, with annotations added.]

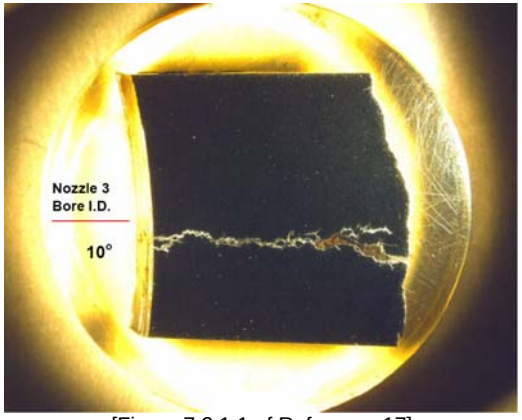

[Figure 7.2.1.1 of Reference 17]

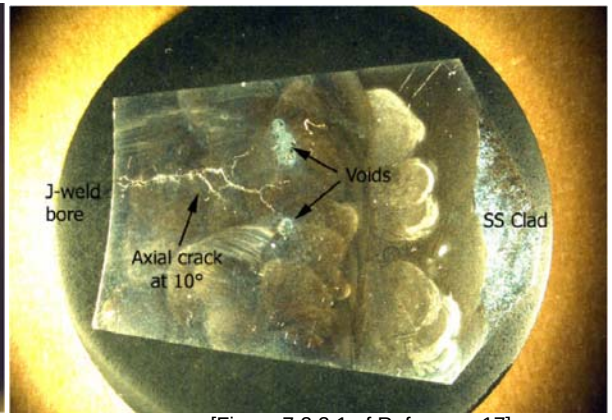

[Figure 7.2.3.1 of Reference 17]

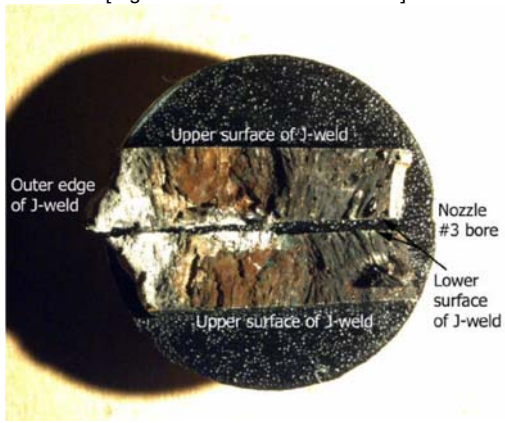

[Figure 7.2.4.1 of Reference 17]

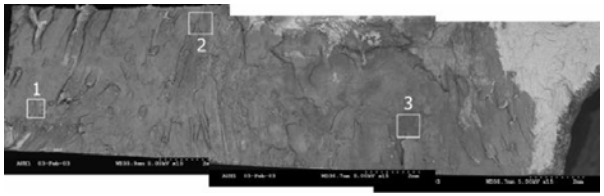

[Figure 7.2.4.6 of Reference 17]

Figure 8.11 BWXT photographs from metallurgical examination of Davis-Besse Nozzle 3 J-groove weld showing extent of PWSCC Crack 1 into weld. [Excerpted from Reference 17]

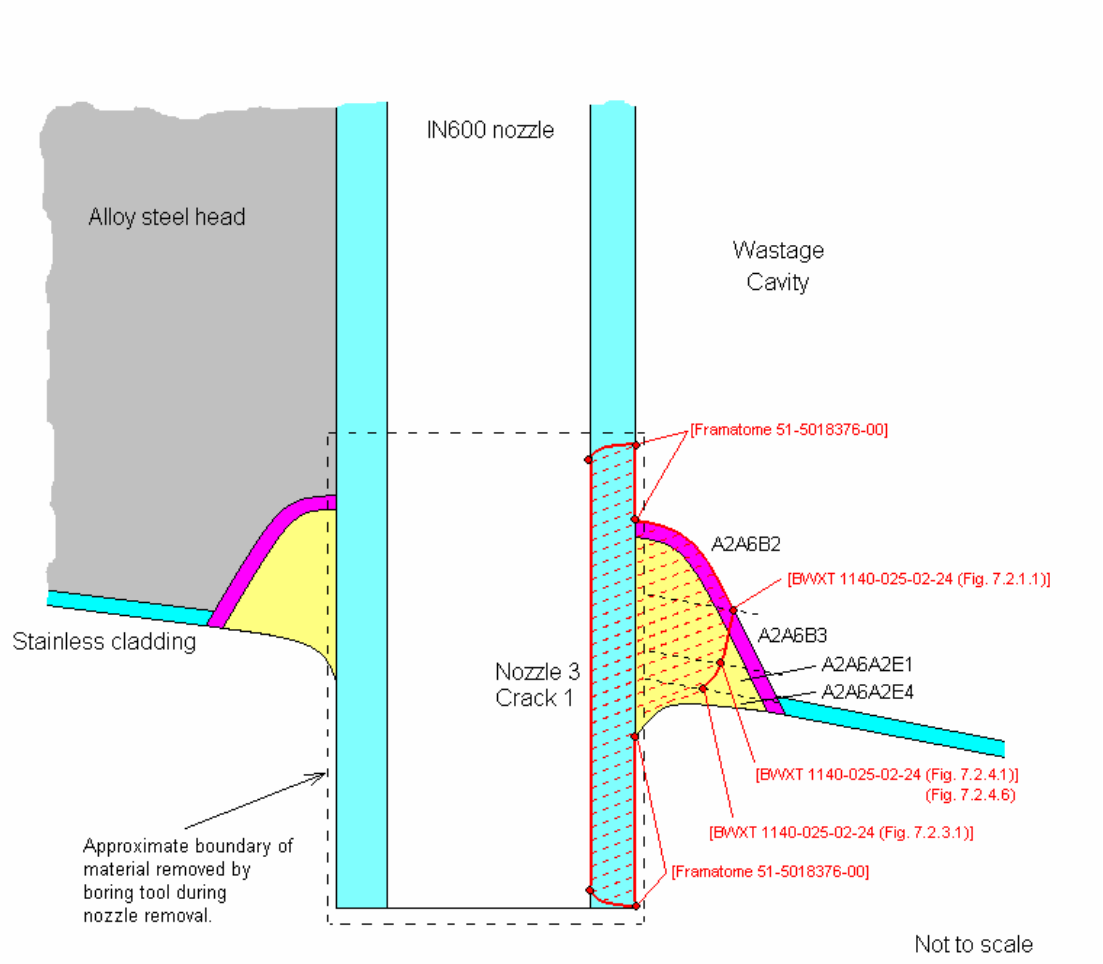

Figure 8.12 Schematic of final size and shape of Crack 1 in Davis-Besse CRDM Nozzle 3 developed from Framatome UT test records [45] and BWXT metallurgical sections [17].

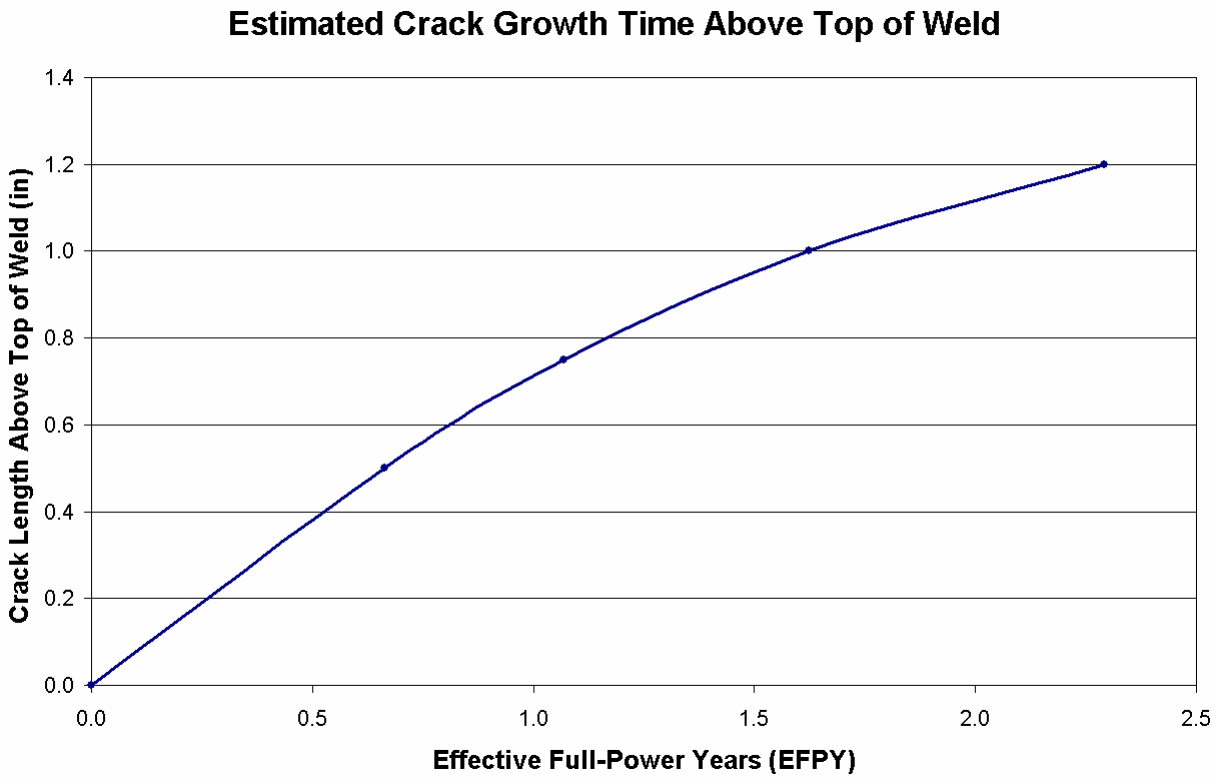

Figure 8.13 Approximate time in effective full-power years (EFPY) to grow the upper tip of a long axial crack in Nozzle 3 to various heights above the top of the weld.

Table 8.1. Axial PWSCC Crack Dimensions in Davis-Besse CRDM Nozzle 2 for Cracks Extending Above the Top of the J-groove Weld

Crack Number	Percent Thru-wall	Axial PWSCC Crack Lengths (inches)		
		OD Total	OD Above Weld	Effective Crack Length for Leakage [a]
1	64	2.33	0.58	0.32
2	100	3.86	0.82	0.82
4	100	2.71	0.47	0.04
6	100	2.59	0.57	0.57
8	100	3.95	1.15	0.24 [b]
10	100	3.04	0.47	0.46 [b]
13	100	3.21	0.76	0.76

[a] Effective crack length for leakage is the distance from the top of the weld to the closest point on the crack front in the nozzle wall, which is the narrowest throat through which leakage flow must pass to reach the annulus.

[b] The small wastage cavity at Nozzle 2 was located above and between Cracks 8 and 10.

Table 8.2. Axial PWSCC Crack Dimensions in Davis-Besse CRDM Nozzle 3 for Cracks Extending Above the Top of the J-groove Weld

Crack Number	Percent Thru-wall	Axial PWSCC Crack Lengths (inches)		
		OD Total	OD Above Weld	Effective Crack Leak Length [a]
1	100	4.08	1.23	1.13
4	100	3.54	0.58	0.39

[a] Effective crack length for leakage is the distance from the top of the weld to the closest point on the crack front in the nozzle wall, which is the narrowest throat through which leakage flow must pass to reach the annulus.

8.6 References

1. ASM Handbook, Volume 13, *Corrosion*, ASM International, 1987.

2. H. Coriou et al, "Corrosion Fissurant sous Contraine de l'Alloy dans l'Eau 'Houte Temperature," presented at 3rd Metallurgy Colloquium, Saclay, June 29-30 and July 1, 1959, North Holland Publishing Co., 1960.

3. "Primary Water Stress Corrosion Cracking (PWSCC) of Alloy 600," Information Notice 90-10, U.S. Nuclear Regulatory Commission, February 23, 1990.

4. "PWSCC of Alloy 600 Materials in PWR Primary System Penetrations," EPRI TR-103696, Electric Power Research Institute, Palo Alto, CA, July 1994.

5. "U.S. Plant Experience With Alloy 600 Cracking and Boric Acid Corrosion of Light-Water Reactor Pressure Vessel Materials," NUREG-1823, U.S. Nuclear Regulatory Commission, April 2005.

6. "Crack Growth of Alloy 182 Weld Metal in PWR Environments (PWRMRP-21)," EPRI TR-1000037, Electric Power Research Institute, Palo Alto, CA, June 2000.

7. "Safety Evaluation for B&W-Design Reactor Vessel Head Control Rod Drive Mechanism Nozzle Cracking," BAW-10190P, B&W Nuclear Technologies, May 1993.

8. "PWSCC of Alloy 600 Materials in PWR Primary System Penetrations," EPRI TR-103696, Electric Power Research Institute, Palo Alto, CA, July 1994**.**

9. "Davis-Besse CRDM Stress Analysis," Calculation No. C-3206-00-1, Revision 0, Dominion Engineering, Inc., November 1, 2001, Attachment 4 to "Supplemental Information in Response to the November 28, 2001 Regarding the Davis-Besse Nuclear Power Station Response to NRC Bulletin 2001-01," Serial No. 2747, Docket No. 50-346, FirstEnergy Nuclear Operating Company, November 30, 2001.

10. "PWSCC of Alloy 600 Materials in PWR Primary System Penetrations," EPRI TR-103696, Electric Power Research Institute, Palo Alto, CA, July 1994.

11. J. Broussard and D. Gross, "Welding Residual and Operating Stress Analysis of RPV Top and Bottom Head Nozzles," *Proceedings of the Conference on Vessel Penetration Inspection, Crack Growth and Repair*, NUREG/CP-0191, U.S. Nuclear Regulatory Commission, September 2005.

12. D. Rudland et al., "Analysis of Weld Residual Stresses and Circumferential Through-Wall Crack K-solutions for CRDM Nozzles," *Proceedings of the*

Conference on Vessel Penetration Inspection, Crack Growth and Repair, NUREG/CP-0191, U.S. Nuclear Regulatory Commission, September 2005.

13. MSC.Marc, Version 2005 r3, MSC Software Corporation, Santa Ana, CA, 2006.

14. D. Rudland et al., "Analysis of Weld Residual Stresses and Circumferential Through-Wall Crack K-solutions for CRDM Nozzles," *Proceedings of the Conference on Vessel Penetration Inspection, Crack Growth and Repair*, NUREG/CP-0191, U.S. Nuclear Regulatory Commission, September 2005.

15. "Root Cause Analysis Report: Significant Degradation of the Reactor Pressure Vessel Head," CR 2002-0891, Rev. 1, First Energy Nuclear Operating Company, August 27, 2002, Section 3.2.1 at page 16.

16. Ibid, Section 3.2.1 at page 14.

17. "Final Report: Examination of the Reactor Vessel (RV) Head Degradation at Davis-Besse," Report No. 1140-025-02-24, BWXT Services, Inc., June 2003.

18. "Root Cause Analysis Report: Significant Degradation of the Reactor Pressure Vessel Head," CR 2002-0891, Rev. 1, First Energy Nuclear Operating Company, August 27, 2002, Section 2.1 at page 2.

19. ASME Boiler and Pressure Vessel Code, 2001 Edition, Section II, "Materials," Part D, "Properties", American Society of Mechanical Engineers, 2001.

20. "Final Report: Examination of the Reactor Vessel (RV) Head Degradation at Davis-Besse," Report No. 1140-025-02-24, BWXT Services, Inc., June 2003.

21. "PWSCC of Alloy 600 Materials in PWR Primary System Penetrations," EPRI TR-103696, Electric Power Research Institute, Palo Alto, CA, July 1994.

22. J. Broussard and D. Gross, "Welding Residual and Operating Stress Analysis of RPV Top and Bottom Head Nozzles," *Proceedings of the Conference on Vessel Penetration Inspection, Crack Growth and Repair*, NUREG/CP-0191, U.S. Nuclear Regulatory Commission, September 2005.

23. D. Rudland et al., "Analysis of Weld Residual Stresses and Circumferential Through-Wall Crack K-solutions for CRDM Nozzles," *Proceedings of the Conference on Vessel Penetration Inspection, Crack Growth and Repair*, NUREG/CP-0191, U.S. Nuclear Regulatory Commission, September 2005.

24. J. Broussard and D. Gross, "Welding Residual and Operating Stress Analysis of RPV Top and Bottom Head Nozzles," *Proceedings of the Conference on Vessel*

Penetration Inspection, Crack Growth and Repair, NUREG/CP-0191, U.S. Nuclear Regulatory Commission, September 2005.

25. D. Rudland et al., "Analysis of Weld Residual Stresses and Circumferential Through-Wall Crack K-solutions for CRDM Nozzles," *Proceedings of the Conference on Vessel Penetration Inspection, Crack Growth and Repair*, NUREG/CP-0191, U.S. Nuclear Regulatory Commission, September 2005.

26. *Ibid*.

27. *Ibid*.

28. "Safety Evaluation for B&W Design Reactor Vessel Head Control Rod Drive Mechanism Nozzle Cracking", BAW-10190P, May 1993, at page 9.

29. *Ibid*, at page 10.

30. *Ibid*, at page 1.

31. "Root Cause Analysis Report: Significant Degradation of the Reactor Pressure Vessel Head," CR 2002-0891, Rev. 1, First Energy Nuclear Operating Company, August 27, 2002, Section 2.1 at page 2, Section 3.2.1 at page 11.

32. "Safety Evaluation for B&W Design Reactor Vessel Head Control Rod Drive Mechanism Nozzle Cracking", BAW-10190P, May 1993, Section 2.4.1 at page 15.

33. *Ibid*, Section 2.4.2 at page 15

34. *Ibid*, Section 2.4.3 at page 17.

35. BWOG materials Committee report BAW-2301, "B&WOG Integrated Response to Generic Letter 97-01: Degradation of Control Rod Drive Mechanism Nozzle and Other Vessel Closure Head Penetrations", July 1997.

36. First Energy letter to the NRC dated January 14, 1999, with Enclosures 1 through 7 (Enclosure 3, Items 1 through 4 contained information specifically applicable to all B&W plants, including Davis-Besse), Enclosure 1, pages 1-6.

37. "PWR Materials Reliability Program Response to NRC Bulletin 2001-01 (MRP-48)," ERPI report 1006284, August 2001, Table 2-1 at page 2-5.

38. "Root Cause Analysis Report: Significant Degradation of the Reactor Pressure Vessel Head," CR 2002-0891, Rev. 1, First Energy Nuclear Operating Company, August 27, 2002, Section 3.2.1 at page 18.

39. B. Alexandreanu et al., "Crack Growth Rates in a PWR Environment of Nickel Alloys from the Davis-Besse and V.C. Summer Power Plants," NUREG/CR-6921, U.S. Nuclear Regulatory Commission, November 2006.

40. *Ibid*, "Executive Summary" at page xv.

41. M. Hacker, "Davis-Besse 13RFO CRDM Nozzle Examination Report", Framatome ANP report 51-5018466-00, Revision 2, May 13, 2002.

42. "Final Report: Examination of the Reactor Vessel (RV) Head Degradation at Davis-Besse," Report No. 1140-025-02-24, BWXT Services, Inc., June 2003.

43. "Root Cause Analysis Report: Significant Degradation of the Reactor Pressure Vessel Head," CR 2002-0891, Rev. 1, First Energy Nuclear Operating Company, August 27, 2002.

44. M. Hacker, "Davis-Besse 13RFO CRDM Nozzle Examination Report", Framatome ANP report 51-5018466-00, Revision 2, May 13, 2002.

45. M. Hacker, "Davis-Besse CRDM Crack Profiles," Framatome ANP Engineering Information Record No. 51-5018376-00, May 13, 2002.

46. M. Hacker, "Davis-Besse 13RFO CRDM Nozzle Examination Report", Framatome ANP report 51-5018466-00, Revision 2, May 13, 2002, page 21 of 69.

47. "Final Report: Examination of the Reactor Vessel (RV) Head Degradation at Davis-Besse," Report No. 1140-025-02-24, BWXT Services, Inc., June 2003.

48. M. Hacker, "Davis-Besse CRDM Crack Profiles," Framatome ANP Engineering Information Record No. 51-5018376-00, May 13, 2002.

49. "Final Report: Examination of the Reactor Vessel (RV) Head Degradation at Davis-Besse," Report No. 1140-025-02-24, BWXT Services, Inc., June 2003.

50. "Material Reliability Program Reactor Vessel Closure Head Penetration Safety Assessment for U.S. PWR Plants (MRP-110): Evaluations Supporting the MRP Inspection Plan", EPRI report (draft final) 1007830, March 2004, Table 4-2.

51. *Ibid*, Table 4-3.